A&A 565, A73 (2014)
DOI: 10.1051/0004-6361/201322938

Astronomy & Astrophysics

Emission lines and shock waves in RR Lyrae stars

D. Gillet[1] and A. B. Fokin[2]

[1] Observatoire de Haute-Provence – CNRS/PYTHEAS/Université d'Aix-Marseille, 04870 Saint Michel l'Observatoire, France
e-mail: denis.gillet@oamp.fr
[2] Institute for Astronomy of the Russian Academy of Sciences, 48 Pjatnitskaja, 109017 Moscow, Russia
e-mail: fokin@inasan.ru

Received 29 October 2013 / Accepted 21 February 2014

ABSTRACT

Context. Emission lines observed in radially pulsating stars are thought to be produced by atoms de-exciting after being excited by a shock wave that is traveling into and then compressing, heating, and accelerating the atmospheric gas.
Aims. With the help of recent observations, we examine the origin of all the different types of emission lines of hydrogen and helium that appear during a pulsation cycle.
Methods. To analyze the physical origin of emission lines, we used the different models of atmospheric dynamics of RR Lyrae stars that have been calculated so far.
Results. In contrast to a recent explanation, we propose that the redshifted emission component of Hα, which occurs near the pulsation phase 0.3, is produced by the main shock. In this case, the emission is the natural consequence of the large extension of the expanding atmosphere. Therefore, this (weak) emission should only be observed in RR Lyrae stars for which the main shock will propagate far enough from the photosphere. It appears as a P-Cygni type profile. We estimate the shock front velocity during the shock propagation in the atmosphere and show that it decreases by 40% when the Hα emitting-shock passes from the photospheric level to the upper atmosphere. The Hα P-Cygni profile observed in long-period Cepheids also seems to be caused by the main shock wave. Although to date He II has only been detected in some Blazhko stars, a comprehensive survey of RR Lyrae stars is necessary to confirm this trend, so we can say that the most intense shocks will only be observed in Blazhko stars.
Conclusions. The development of a model of atmospheric pulsation that takes the effects of 2D and 3D convection into account, seems to be a necessary step to fully quantify the effects of shock waves on the atmospheric dynamics of radially pulsating stars.

Key words. stars: variables: RR Lyrae – stars: variables: Cepheids – stars: atmospheres – shock waves

1. Introduction

Recently, the CoRoT and *Kepler* missions have delivered photometric data of unprecedented precision, leading to spectacular results for RR Lyrae stars (Kolenberg 2013). On the other hand, ever since the use of photographic plates, the quality and accuracy of spectroscopic observations continue to advance. However, despite more than a century of observations since the discovery of RR Lyrae stars, the emission of helium has only recently been discovered (Preston 2009, 2011). We have known for several decades that a component of the hydrogen emission occurs just before maximum brightness. For Hα, its maximum intensity rarely exceeds 25% of the continuum. We are far from the factor of 10 or 20 above the continuum, as observed in Miras stars.

A secondary Hα emission (called the "second apparition" by Preston) has been discovered by Gillet & Crowe (1988) during the pre-minimum brightening near the pulsation phase $\varphi = 0.72$. It is produced when outer atmospheric layers in ballistic infall collide with inner, more slowly photospheric layers. A third weak emission (the "third apparition") has been recently observed in the red absorption wing of the Hα profile by Preston (2011). Its physical origin has not yet been identified. Finally, there are three emission episodes within the Hα profile during one pulsation cycle.

It is now well accepted that the brightest emission observed during the main acceleration phase of the atmosphere is produced in the radiative wake of a shock wave propagating through the atmosphere. This shock forms below the photosphere near the time of minimum radius and suddenly accelerates outward. It is very strong and stops the (supersonic) infall of matter during its rise in the atmosphere. A weak hydrogen emission can be induced during the collision of the highest infalling atmospheric layers with the deepest ones. Thus, a shock/presure wave is sometimes generated, which produces the observed bump on the light curve. Finally, our understanding of the physical origin of all observed emissions can bring us crucial information about shocks and the nonlinear dynamics of radially pulsating atmospheres. Indeed, emission and absorption profiles contain a wealth of information about the atmospheric velocity structure and can be used to obtain some quantitative insight into the stratification of outflowing and infalling material.

The calculation of emission lines that are formed in the radiative wake is a very difficult job. Details of predicted profiles may be affected by inadequate treatment of the shock, the radiative balance, or radiative transfer. Very few researchers have tried to solve this problem in a self-consistent manner. Moreover, when the shock front is far from the photosphere, the thickness of the radiative wake may be noticeable. In this case, photons are formed in a large volume of matter in the outer layers, and this causes a "nebular" emission component to the line profile. Although, in this configuration, the emitted flux may only be weak per unit volume, a reversed P-Cygni-like emission can be observed on the blue side of the absorption component.

In Sect. 2 of this paper, we discuss hydrogen emission lines from the observational point of view. In Sect. 3, we analyze the

occurrence of the different types of shocks from dynamical models of the pulsating atmosphere. The behavior of the main shock associated with the "first apparition" of the Hα emission is discussed in Sect. 4. The physical origin of the "second apparition" and the "third apparition" are discussed in Sects. 5 and 6, respectively. The important case of helium emission lines is examined in Sect. 7. Section 8 is devoted to the origin of the "lump" and the "bulge phenomena", features recently highlighted in the light and radial velocity curves, is discussed in Sect. 9. We discuss the role of the main shock in the Blazhko effect in Sect. 10. Finally, some concluding remarks are given in Sect. 11.

2. Shocks from hydrogen emission lines: observational approach

It is now a well-established fact that hydrogen emission lines are a characteristic feature of radially pulsating stars of various types. The intensity of the hydrogen emission seems to correlate with the amplitude of the pulsation. Indeed, RR Lyr variables only exhibit weak emission lines (Preston 1964) and in classical Cepheids, hydrogen emission lines are scarcely detected (Hutchinson et al. 1975), Unlike Mira type where strong hydrogen emissions are observed. Evidence of shock signatures is based on line doublings and emission in hydrogen lines (Preston & Paczynski 1964; Preston et al. 1965). Moreover, for RR Lyrae stars, observations indicate that the strongest emission is present during a very short time, about 4% of the period in a pulsation cycle.

Following Preston (2011), three moderate-to-small emission components appear successively in the Hα profile during a pulsation cycle (Fig. 1). In order of decreasing intensity and date of discovery, we have the so-called "first apparition" that occurs just before the luminosity maximum. The emission was first detected by Sanford (1949). Its physical origin is attributed to the presence of the hot emitting layer behind an outward-moving shock front, as first proposed by Schwarzschild (1952).

The "second apparition" was discovered by Gillet & Crowe (1988). It occurs during the bump, i.e., around the average pulsation phase $\langle\varphi\rangle = 0.72 \pm 0.02$, average over several different stars which have different bump phases. It is produced when outer atmospheric layers in ballistic infall collide with inner deep layers. The bump was interpreted by Hill (1972) as the consequence of a shock or collision, called "early shock".

The last emission component, the "third apparition", has only recently been discovered (Preston 2011). It is a weak redshifted emission that is observed during declining light and that reaches its maximum strength near pulsation phase $\varphi = 0.30$. It occurs both in Blazhko and non-Blazhko stars. Chadid & Preston (2013) suggest that this emission component is caused by a weakly supersonic and infalling shock wave (called Sh_{PM}, PM for post maximum). They also assumed that this hypothetical shock is associated with the "lump" and the "bulge phenomenon", features recently highlighted in the light and radial velocity curves. Thus, this shock would occur at the beginning of atmospheric compression, i.e., in the early phase of the infalling motion of the atmosphere.

3. Shocks from dynamical models: theoretical approach

Recently, Ludwig & Kucinskas (2012) calculated three-dimensional (3D) hydrodynamical atmosphere models of non-pulsating red giant stars. They find that the lower atmosphere

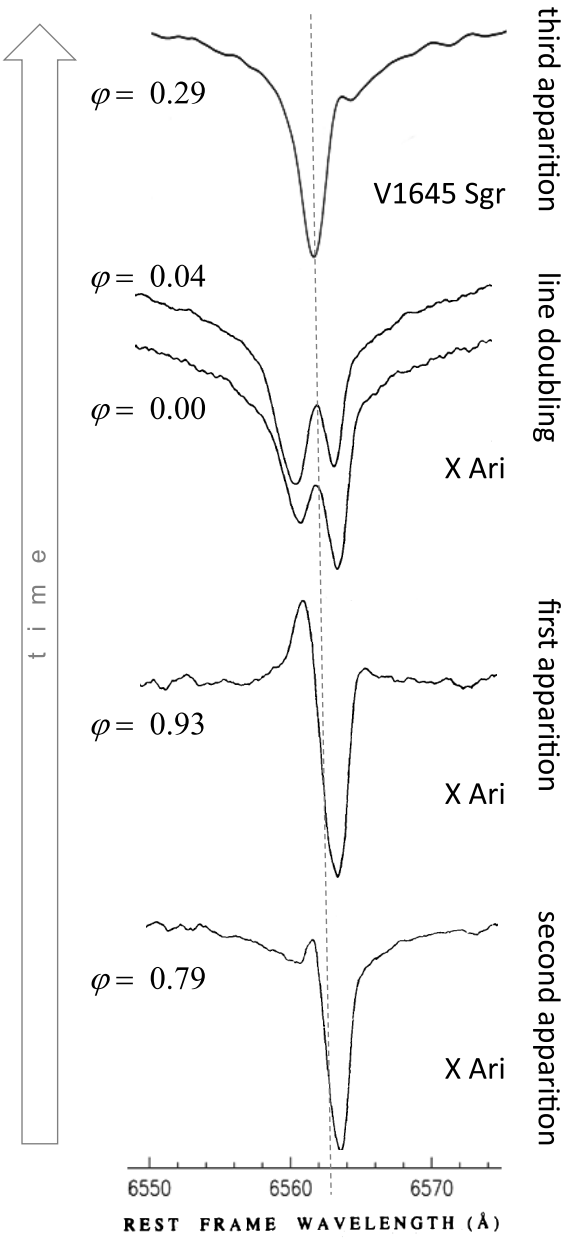

Fig. 1. Observed line profile of the three emission components occurring in the Hα line. They appear successively during a pulsation cycle. The most intense emission was first discovered around the pulsation phase $\varphi = 0.93$. The second was for the first time observed in X Ari by Gillet & Crowe (1988) in the phase interval $\varphi = 0.72-0.82$. The third was detected recently by Preston (2011) in the three RR Lyrae stars: RV Oct, WY Ant and V1645 Sgr, with a maximum strength near phase $\varphi = 0.30$. Currently, there are no observations of X Ari around the phase 0.30. The two first emission components are blueshifted, while the last and weaker one is redshifted. The "apparitions" are classified according to the date of the discovery of the emission line.

is dominated by convective motions and that the upper atmosphere is dominated by wave activity. Thus, fast shock waves, with vertical and horizontal velocities of up to Mach ~2.5 and ~6.0, respectively, frequently traverse the upper atmosphere. Consequently, the 3D structure of these layers (chromosphere), formed by the interaction of shock waves, is complex. In comparison, as shown by Wedemeyer et al. (2004), shocks occurring in the Sun have vertical and horizontal velocities that are significantly weaker (maximum Mach numbers of ~1.5

and ∼1.8, respectively). In these non-pulsating stars, acoustic waves excited by convective motions, propagate upwards, steepening into shocks, dissipate, and deposit their mechanical energy as heat in the upper atmosphere. In radially pulsating stars, vertical shocks govern the atmospheric dynamics of the high atmosphere due to their very fast velocity (hypersonic shocks). Moreover, in this limiting case, shocks dissipate most of their energy by radiation.

Christy (1964) outlined the basic formulation for modeling radial stellar pulsation. His nonlinear calculations use a one-dimensional (1D) Lagrangian framework with a purely radiative envelope. Radiative models had considerable success producing full-amplitude RR Lyrae models, but they are not relevant for identifying the red edge to the RR Lyrae instability strip, because they do not take convection into account. Indeed, convection in the hydrogen and helium ionization zones quenches pulsation (Baker & Kippenhahn 1965). More precisely, convection reduces the growth rate of pulsation but does not produce pulsational stability (for instance, Tuggle & Iben 1973). All 1D models including convection have difficulty reproducing the observed properties for cool RR Lyrae stars. For instance, the red edge is less reliable than the blue edge because of its well known sensitivity to the efficiency of convection and to the uncertianties affecting the treatment of turbulent convection (Marconi 2009). Thus, 1D theoretical attempts to determine a red edge explicitly become an impossible mission. Moreover, 1D models have difficulty matching observed light curves near the red edge. Finally, because convection is a multidimensional phenomenon, 1D models always approximate the effects of convection.

Geroux & Deupree (2011, 2013) are developing a 3D radiation hydrodynamics code of a rather low resolution grid to simulate the interaction of convection and pulsation in large-radial amplitude variable stars such as RR Lyrae. The 3D approach removes the need for many free parameters used by 1D models, because 3D convection results specifically from the conservation laws. Using artificial viscosity may affect the final amplitude of the full-amplitude solution by converting radial pulsation kinetic energy into internal energy. Consequently, shock wave amplitudes may also be affected to some degree. Finally, the current use of models predicting the propagation of shock waves in the atmosphere of high amplitude pulsating stars, including a treatment of convective heat transfer or not, or how elaborate it may be, should be made with caution. Recently, Mundprecht et al. (2013) have extended the ANTARES code to simulate the coupling of pulsation with convection in Cepheid-like variables in multiple dimensions. They demonstrate that with a grid refinement, numerical artifacts no longer occur. Thus, high resolution simulations allow the sizes of grid cells to reasonably correspond to the size of physical features. In particular, strong shock fronts and hydrogen and helium ionization zones can be properly calculated over many pulsation cycles. Consequently, in the coming years, it should certainly be possible to determine the exact role of radiative shocks on atmospheric dynamics of radially pulsating stars.

Recently, Stellingwerf (2013) presented some very interesting preliminary results of RR Lyrae pulsation from his 3D-smooth particle hydrocode (SPHC). In this simple model, pulsation is initiated by applying an initial inward velocity field. First, the 3D approach highlights that the turbulent mixing clearly accelerates during the expansion phase of the pulsation. This is interpreted as the effect of the shock because it compresses the gas layers during its passage through the atmosphere. Consequently, the Richtmyer-Meshkov Instability may be important. The second process identified by the model is the spontaneous generation of a strong, hot, extended shock driven outflow at the upper boundary. The shock resembles the Hill results, with infalling material colliding with each new outgoing shock. Unlike the classical 1D radial shock, this shock is very unstable, with lots of small scale turbulent motion in the shocked material, which is direct consequence of the interaction of pulsation and turbulence. Nevertheless, because this model does not include radiative processes, especially the radiative nature of the shock with its significant radiative losses, these results should be considered preliminary.

Many researchers have found that the main shock is produced by the opacity mechanisms on H and He atoms producing pulsations. It is the main dynamical result of the pulsation mechanism (Whitney 1956a,b). The shock associated to the H-opacity mechanism has a higher intensity than the one based on the He-opacity. During the beginning of their propagation in the lower atmosphere, they merge into a single shock. This quickly gains a very high intensity as the density of the gas sharply decreases with height. This means that the shock accelerates during at least a part of its upward propagation. As for all shocks, the main shock always propagates (in the mass scale) outward. The hydrogen emission in the spectra of pulsating stars is thought to be due to radiative cooling of the gas compressed by the shock propagating through the atmosphere in each pulsation cycle (Abt 1959; Wallerstein 1959).

The first pulsating model exhibiting the development of a shock wave was done for W Virginis by Whitney (1956b). His model was driven by a sinusoidal piston at the base of the photosphere. Because the postshock cooling time is very short, he assumed an isothermal atmosphere for his model, although this idealized case has little in common with the presence of real shocks in a pulsating atmosphere. Christy (1966), then Castor (1967), recalculated a grid of pulsational models of RR Lyrae stars, using finer zoning in the hydrogen ionization region and replaced the diffusion equation by an integral solution for the radiative transport. However, their models do not have enough of an atmospheric extent to calculate fully developed shocks. For the first time, Hill (1972) calculated RRa models with a large enough extended atmosphere to allow a realistic shock-wave development. In the course of pulsation, the extension of the atmosphere increases by 21 times with respect to the static atmosphere. Consequently, the motion of the outer layers is strongly desynchronized unlike the photospheric layers.

Fokin (1992) investigated the Hα formation in the atmosphere of RR Lyrae by simultaneouly solving the hydrodynamical equations and the non-steady transfer equation for the continuum radiation. Moreover, unlike Hill, his model did not use a piston to simulate pulsations, but he considered the κ-mechanism occurring within H- and He-ionization zones. Consequently, his full-amplitude hydrodynamical model can be considered as more appropriate than Hill's approach. The main result about the atmospheric dynamic obtained by Hill and Fokin is the production of two strong shocks during each pulsationnal cycle. There is the well-known "main shock" induced by the κ-mechanism that appears during the beginning of the photospheric expansion. There is also a secondary shock called "early shock" by Hill, which appears above the photosphere during the atmospheric contraction.

Fokin & Gillet (1997) certainly give the best detailled analysis of the physical origin of the different shocks occurring during a pulsation cycle of RR Lyrae. In the published models, the temperature at the inner boundary of each model was between 500 000 K and 900 000 K while the atmosphere contained 40%–50% of the total number of mass zones (from 90

to 150 depending on the model) with a density at the surface as low as 10^{-14} g cm^{-3} (i.e., 10^4 lower than the density at the photospheric level). Thus, the atmospheric extent was sufficient to calculate full developed shocks. However, because the temperature at the inner boundary of these models is relatively cool, it could affect phases in which the shocks occur. Consequently, we have done several test calculations to be sure that the dynamics of the models does not depend on the chosen inner temperature. For instance, with an inner boundary temperature of 500 000 K, the radii of the model RR41 are R(out) = 5.27 $R_\odot$ and R(inner) = 2.2 $R_\odot$. The period is 0.5656 day, and the $\sigma_{\rm imag}$ (the excitation rate) is 0.177×10^{-2}. We calculated the same model with the inner temperature boundary at 2 000 000 K, which gives the following parameters: R(out) = 5.27 $R_\odot$, R(inner) = 0.801 $R_\odot$, the period of 0.5660 day and excitation rate of 0.175×10^{-2}. Thus, the dynamics of the two models are similar.

With their purely radiative models, Fokin & Gillet (1997) found that there are five shock waves per pulsation cycle, including the early and main shocks. However, these five shocks have different amplitudes and different physical origins. In addition to the two main shocks already discussed above, there are three lower amplitude shocks. The first one (s4) appears during the beginning of the atmospheric compression as a consequence of the accumulation of a few weak compression waves generated by the local rarefaction induced by the hydrogen recombination. The second weak shock (s3) is associated with the stop of the hydrogen recombination front near the phase of maximum expansion (see Fokin et al. 1996). Finally, the origin of the third shock s3', which appears after the maximum radius near phase 0.57, is not clear. It seems to be the consequence of a superposition with the transient and very weak 1H-mode with the F-mode. According to Gillet (2013), it is possible that this shock should only be observed in Blazhko stars. Fokin et al. (1996) did not detect this uncommon shock in their model devoted to the classical Cepheid star: δ Cephei. This would mean that in normal pulsating stars, there would be four shock waves of significant intensity by pulsation cycle.

As shown by Fokin & Gillet (1997), all these shocks merge together in the high atmosphere to form the main shock that produces the strongest observed Hα emission near the pulsation phase 0.92, i.e., just before the luminosity maximum. The Mach number of shocks s4 and s3 is too small (<3) to induce any Hα emission component.

4. The shock associated to the "first apparition" of Hα emission

In general, hydrogen emission lines are produced in the shock wake, that is a relatively narrow region behind the shock front, except when the shock reaches the highest part of the atmosphere. In this case, when the shock is far away from photosphere, the thickness of the wake can be very large. Thus, the simple calculation of steady-state, plane-parallel radiative shock waves propagating through the atmospheric gas is not sufficient to fully describe emission lines. All thermodynamical and dynamical processes occurring in the stellar envelope must be understood as a whole, along with the pulsation and the various spectral signatures observed.

However, in the restrictive context of the steady-state, plane-parallel approach, Fadeyev & Gillet (2004) considered a shock wave propagating through a homogeneous medium consisting solely of atomic hydrogen atoms with the five first bound levels and the continuum. They solved the transfer equation for the whole shock wave structure (precursor and wake) in the comoving frame for hydrogen lines, whereas the continuum radiation was calculated for the static medium to overcome the numerical instability arising at the velocity discontinuity. Indeed, it appears that the role of the radiation field in spectral lines is must less that in the continuum. Furthermore, the Doppler shifts in the hydrogen lines do not perceptibly affect either the structure or the radiative losses of the shock wave.

One of the most remarkable results found by Fadeyev & Gillet (2004) is that the shock wave model reveals a double emission structure in Hα and Hβ profiles, whereas profiles of higher Balmer lines only exhibit the asymmetry. This result is quite consitent with high resolution spectroscopic observations of the strong hydrogen emissions in Mira, W Virginis, and RV Tauri stars (see references in Fadeyev & Gillet 2004). The redshifted emission component, if we take the infalling motion of the high atmosphere into account, comes from photodeexcitations occurring in the radiative precursor just ahead of the discontinuous jump, while the gas producing the blueshifted emission component is located in the hydrogen recombination zone of the wake.

The double structure in emission is not observed in RR Lyrae stars and classical Cepheids. Indeed, for these two types of pulsating stars, the profile of hydrogen lines is completely dominated by the broad atmospheric absorption. Moreover, the observed emission component in the Balmer lines is weaker, narrower, and much more fleeting than in Mira, W Virginis, and RV Tauri stars. These differences between emission behaviors were first discussed by Castor (1972). In addition, Fokin (1992) showed that the lack of strong Hα emission in RR Lyrae stars is due to the high altitude formation of the line in the atmosphere. Indeed, it appears that the full development of the main shock only occurs far above the photosphere in contrast to Mira, W Virginis, and RV Tauri stars. This means that Balmer emissions may not be observed when the shock first emerges in the photosphere. The shock evidently forms at this level, but its Mach number is too low to induce a significant emission. The absence of Balmer emissions in almost all short-period Cepheids (smaller than 10 days) must be caused by this phenomenon.

Often the absorption component in the Balmer profile is not visible in Mira, W Virginis, and RV Tauri stars. Only a broad emission line is observed. In contrast, the small emission peak in the Balmer lines in RR Lyrae stars is narrower than the broad absorption component. Because the shock reaches its full amplitude in the highest layers of the atmosphere, the emission is formed in the low density gas behind the shock front. Under these conditions of rarefaction, the optical thickness of the formation region of the Hα emission in the radiative wake does not exceed 100 (Fokin 1992), which gives a narrow emission width close to isothermal conditions. This width is several times smaller than those taking place in Mira, W Virginis, and RV Tauri stars (Fokin 1991).

Fadeyev & Gillet (2004) found that the Doppler shift in Balmer emission lines is roughly one third of the shock front velocity $V_{\rm shock}$ in the frame of the observer for gas densities of 10^{-12} g cm $\leq \rho_1 \leq 10^{-9}$ gm cm. The upstream Mach numbers range within $6 \leq M_1 \leq 14$ and a preshock temperature of $T_1 = 3000$ K,

$$V_{\rm shock} \cong 3c\frac{(\lambda_{\rm e} - \lambda_0)}{\lambda_0} \quad (1)$$

where $\lambda_{\rm e}$ is the wavelength of the maximum intensity of the Hα emission and λ_0 the laboratory wavelength.

It is assumed that the line-of-sight motion of the star with respect to the observer has already been corrected. Moreover,

they showed that the gas flow velocity of the gas emitting the Balmer line radiation is approximately one half of the shock wave velocity in the frame of the observer. These interesting results can lead to a good estimate of the shock front velocity from observed Balmer profiles. For instance, from the high resolution Hα profiles reported by Gillet et al. (2013), we obtain a front velocity of 117 km s^{-1} at $\varphi = 0.911$, which is the pulsation phase of the maximum intensity of the Hα emission. This estimate is given in the frame of the observer. Because the emission is less and less blueshifted when the pulsation phase increases, this means that the shock front velocity decreases when the shock propagates above the photosphere. Its velocity varies from 132 km s^{-1} at $\varphi = 0.902$ to 114 km s^{-1} at $\varphi = 0.927$. Beyond this stage, because of the significant increase in the blueshifted absorption component, it is difficult to estimate how the shock is weakening when the shock begins to cross the highest layers of the atmosphere. Because the infall velocity is not zero, the shock front velocity deduced from observation actually corresponds to the shock amplitude. Thus, an estimate should be made of the infall velocity to know the real speed of the shock front in the stellar frame. However, when the pulsation amplitude becomes large, the motions of the atmosphere are very complex and highly variable from one cycle to the next. Consequently, although this estimate can be done in principle, given the phase of pulsation and a hydrodynamic model, the result is uncertain in such a calculation. Only an observational estimate seems the best.

5. The shock associated to the "second apparition" of Hα emission

Hill (1972) showed that the early shock forms as the star is still contracting, although the shock is moving outward in mass. Because the intensity of shocks s4 and s3 are too low (Fokin & Gillet 1997) and the bump in the light curve is also observed in non-Blazhko stars, the shock s3' cannot be the cause of the "second apparition" of Hα emission. Consequently, the physical origin of this emission could be the result of collision between the layers of the upper atmosphere with the photospheric layers during the in-fall phase of the ballistic motion. Depending on stellar parameters, the pulsation phase of this collision, i.e., that of the bump ($\langle\varphi\rangle = 0.72 \pm 0.02$), is variable from one non-Blazhko RRab star to another, as reported by Gillet & Crowe (1988). For Blazhko stars, the bump emergence also depends on the Blazhko phase. When the Blazhko effect is active, the shock s3' may induce an earlier or later occurrence of the bump. This means that a displacement of the collision region occurs over the Blazhko cycle. Finally, it is when the shock front s4+s3 has already reached a Mach number greater than 5, around the pulsation phase 0.72, that the collision with the photospheric layers occurs. The star is near its minimum radius, and just before that the shocks s2 and s1 emerge from the photosphere and abruptly begin to reverse the motion of atmospheric layers.

6. The shock associated to the "third apparition" of Hα emission

Chadid & Preston (2013) provide an explanation about the "third apparition" of Hα emission. They interpret it as due to the presence of a shock wave Sh_{PM}, which is a superposition of the compression due to the hydrogen recombination front and an accumulation of weak compression waves. They assume that the intensity of Sh_{PM} could be high enough to produce the weak redshifted emission observed in the Hα profiles of RV Oct, WY Ant, and V1645 Sgr around $\varphi = 0.30$.

When the hydrogen recombination front (HRF) stops its inward motion because of ever-growing density, at this moment the velocity discontinuity at the HRF transforms into two running waves moving in the opposite directions (see Fokin et al. 1996). This hydrodynamical phenomenon is observed around the pulsation phase ($\varphi \approx 0.30$). Consequently, the progressive steepening of the wave in the upward direction and its transformation into a shock wave occurs later at phase $\varphi \approx 0.40$. In this phase, the intensity of the shock (called s3 by Fokin et al. 1996) is very weak (Mach number between 1.5 and 2). This means that it cannot produce hydrogen in emission. Therefore, the weak redshifted emission within the Hα profile first observed by Preston (2011), cannot be explained by such a weak shock.

There is another plausible mechanism, still based on the existence of a shock wave. The redshifted emission occurs when the shock is detached from the photosphere. In this case, the emission is a P-Cygni like profile that is the signature of an expanding envelope surrounding the stellar surface. This type of profile characterizes the difference between stars with normal and extended atmospheres. Three radiative outflows can be distinguished: (1) the "early stage" when the emission is blueshifted; (2) a transition phase, the "intermediate stage", which occurs when the shock detaches from the photosphere; and (3) the "late stage" when the emission appears "redshifted" (P-cygni profile), i.e., when the shock reaches the very high atmosphere, the stellar envelope (Fig. 2). In the intermediate stage, the emission is blended with the broad absorption. Moreover, if the emission intensity is not strong enough as in RR Lyrae stars, the profile only appears in absorption, often with a double structure due to the Schwarzschild's mechanism (Schwarzschild 1952). Thus, at the beginning of this stage, the absorption can be severely affected by the filling of the emission component.

Classically, in an extended atmosphere, P-Cygni profiles occur when a supersonic atmosphere (wind) surrounds a continuum source (photosphere). Thus the expanding atmosphere absorbs continuum photons from the photosphere. Moreover, in a normal P-Cygni profile, a spherically symmetric envelope is considered that is radially expanding away from the stellar photosphere. For this basic configuration, the expanding atmosphere produces both a broad emission line and a blueshifted absorption of the continuum photons. In RR Lyrae stars, we have a variant case: the expanding atmosphere is replaced by a radiative shock wave, thus the radiative outflow is localized in a shell with a supersonic expanding velocity. In general, the thickness of the radiative shock wake is much smaller than the whole atmosphere. Moreover, because the volume of the emitting layer at any frequency decreases with increasing flow velocity, especially in the case of a shock, the geometrical thickness of the shell producing the specific profile increases with decreasing density. This case is more like to the formation of P-Cygni line profiles in T Tauri stars and type II SN outflows than in expanding envelopes of late-type giants or supergiants in the sense that part of the atmospheric gas is excited (expanding gas shell). On the other hand, it is not necessary that a shock wave is present in the atmosphere to observe a P-Cygni profile, as is the case in some hot stars. In fact, the shock allows the gas located in its wake to reach a temperature high enough to produce the emission of photons.

The classical P-Cygni profile refers to an optically-thin medium except in the neighborhood of spectral lines. Thus, emission photons can occur throughout the whole envelope. The separation between the minimum of the absorption and the maximum of the emission gives the terminal velocity of the

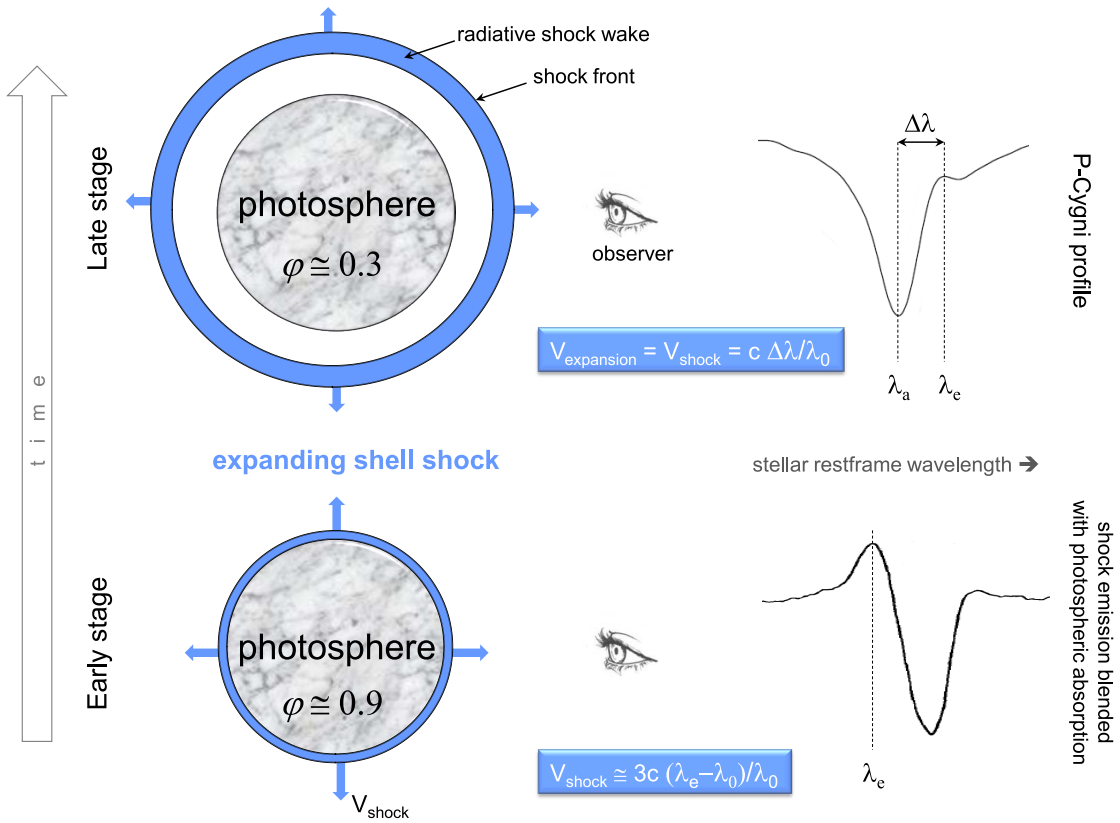

Fig. 2. Hypothetical scheme of evolution of the Hα line profile when the main shock wave propagates in the envelope of an RR Lyrae star. The early stage occurs just before the luminosity maximum (pulsation phase 0.9), i.e., when the shock front is close to the photosphere. During the late stage (pulsation phase around 0.3), a P-Cygni profile is observed. It means that the shock front is detached from the photosphere. The expanding shell is actually the radiative wake of the shock in which the Hα emission line is formed. λ_e is the wavelength of the maximum intensity of the Hα emission, λ_a is the wavelength of the minimum intensity of the Hα absorption and λ_0 the laboratory wavelength.

expanding gas. When the emission is induced by a shock wake, the terminal velocity is the shock front velocity

$$V_{\rm shock} \cong c\frac{(\lambda_{\rm a} - \lambda_{\rm e})}{\lambda_0} \quad (2)$$

where $\lambda_{\rm a}$ is the wavelength of the minimum of the Hα absorption and $\lambda_{\rm e}$ the wavelength of the Hα emission. For the profiles of RV Oct, WY Ant, and V1645 Sgr, for which Chadid & Preston (2013) report detecting the weak redshifted emission, we obtain shock velocities of 76, 73, and 85 km s^{-1}, respectively. These velocities remain constant during the visibility of the emission, around $\varphi = 0.30$.

These estimates show that the velocity of the main shock decreases by 40% between the luminosity maximum and the occurrence of the P-Cygni profile. If we take an average velocity of propagation of the shock equal to 100 km s^{-1} during about 40% of the pulsation period, the shock travels a distance greater than 50% of the photospheric radius. Thus, at the pulsation phase $\varphi = 0.30$, the shock is detached well from the photosphere. This result is consistent with our hypothesis of a P-Cygni profile, i.e., a line profile formed far away from the photosphere.

Nardetto et al. (2008) present HARPS high resolution spectroscopy ($R = 120\,000$) with a high $S/N = 300$ of eight galactic Cepheids with periods between $P = 3.39$ d and $P = 41.52$ d. Long-period Cepheids present Hα emission components that might be explained by the presence of a shock wave propagating in the upper atmosphere of the star. A circumstellar shell helps us to understand the complex dynamical structure of long-period Cepheids. Thus, many of these stars, if not all, could be surrounded by warm circumstellar envelopes created by mass loss. Baldry et al. (1997) and Nardetto et al. (2008) show that the Cepheid ℓ Carinae ($P = 35.6$ d) exhibits two narrow Hα emissions per a pulsation cycle. There is a blueshifted one that appears at $\varphi = 0.70$ and disappears just before the luminosity maximum at $\varphi = 0.90$ (see their 2D-Fig. 4). It reaches its intensity maximum at $\varphi = 0.84$.

The second emission component is redshifted. It appears just after the luminosity maximum, and its intensity and velocity decrease until $\varphi = 0.50$ with a maximum near $\varphi = 0.08$. We find the same pattern as observed in RR Lyrae stars. If we accept that the profile showing the redshifted emission is a P-Cygni type profile, then we can deduce a decreasing shock front velocity from 100 to 70 km s^{-1} between the pulsation phases 0.0 and 0.50. From the blueshifted emission, we obtain a shock front velocity of 162 km s^{-1}. With an average shock front velocity of 125 km s^{-1} and an observability during 80% of the period, the shock front would go up more than two stellar radii away. Thus, the shock propagates very far beyond the photosphere, unlike RR Lyrae stars. This may therefore explain why the emission components are narrower in the case of Cepheids. Moreover, as the redshifted emission is no longer observed from $\varphi = 0.50$, we expect that in the low density part of the high atmosphere in which the shock is propagating, a shock front velocity higher than 70 km s^{-1} is required to induce hydrogen emission.

Finally, in our interpretation, the "third apparition" of Hα emission during a pulsation cycle would simply correspond to the final propagation stage of the main shock in the high

atmosphere. It is redshifted, but in fact characterizes the outward motion of the shock, which is detached from the photosphere.

7. Helium emissions in RR Lyrae stars

Preston (2009, 2011) was the first to observe He I lines in emission during rising light in ten RRab stars. The strongest emission was He I λ5875.66 (D3), and a weaker emission was also detected on He I λ6678.16 (singlet). He I emissions were observed both in Blazhko and non-Blazhko stars. Until now, only He II was detected in Blazhko stars. It should be noted that Gillet et al. (2013) and Gillet (2013) mistakenly reported that no emission lines of helium were observed in non-Blazhko stars instead of saying only He II.

Using the classical Rankine-Hugoniot equations, just after the viscous shock front, the postshock temperature is extremely high, up to 10^5–10^6 K depending on the shock Mach number, typically between 10 and 30. Then, during the thermalization between electrons and heavy particles, the temperature quickly decreases to a few tens of thousands of degrees. At that time, ionizations and excitations by electronic collisions occur. They are followed by recombinations and de-excitations that produce the observed emission lines. In this radiative region of the shock wake, the gas density is typically 50 to 100 times that of the unperturbed gas in front of the shock (Fadeyev & Gillet 2001). If the shock Mach number is high enough, the temperature and the density in the de-excitation region of the wake could be sufficient to produce He I and He II emission lines. These emissions occur in a relatively narrow shell with respect to the thickness of the atmosphere. Hydrogen emission lines are formed just after helium lines, in a slightly colder region of the shock wake. An example of the structure of the radiative shock wave occurring in radially pulsating stars is given by Fadeyev & Gillet (2004). The thickness of the hydrogen and helium emitting shell is less than a few kilometers when the unperturbed gas density is 10^{-10} g cm^{-1}. Of course, when the shock reaches the upper atmosphere, the gas density decreases rapidly, and accordingly, the shell thickness may be much larger.

Thus, the presence of helium emissions depends on the intensity of the shock wave. The He I emission lines served to confirm that the temperature behind the shock is sufficient to ionize He once, while the He II shows that the temperature has exceeded a critical threshold. Thus, it is possible to determine the critical amplitude of the shock required to produce He II emission. This observational information is very useful for modeling the main shock. If a shock amplification mechanism occurs in Blazhko stars (Gillet 2013), we expect that there are stronger shocks in Blazhko stars than in non-Blazhko stars. Today, observations suggest that the intensity of shock waves occurring in non-Blazhko stars is not strong enough to produce He II emission. However, it is possible that in the future, we detect He II emission in some non-Blazhko stars with stellar parameters (radius, mass, etc.) outside the norm. In this case, shocks occurring in these stars would be of exceptional intensity.

The Blazhko star S Ara is the one of largest amplitude RRab stars with a V-magnitude between 10.042 and 11.506 (HIPPARCOS light curve). Upon careful inspection of UVES and HARPS spectra of S Ara, Chadid (2011) claims to have detected helium emission lines during rising light of this star. She presents a first UVES-plot (see her Fig. 5) for He I lines 4028.18 Å and 4471.48 Å between pulsation phases 0.96 and 1.08, and a second HARPS-plot (see her Fig. 6) for the classical He I lines 5875.62 Å and 6678.15 Å between pulsation phases 0.81 and 1.14. The wavelength scale is given in the stellar rest frame wavelength. Curiously, from these plots, helium emission never appears, especially around the phase of maximum luminosity.

Moreover, she also states having observed a weak emission of the single ionized helium line He II $\lambda\lambda$4686 in S Ara. An emission appears only once at phase 0.93 (see her Fig. 7). Thus, it is not possible to confirm it on other spectra taken just before or after it, such as Preston (2011) did for AS Vir (see his Fig. 9). The FWHM of the Chadid's emission is very narrow (0.1 Å), close to the instrumental width of the spectrograph used (UVES, R = 45 000). Moreover, a similar narrow emission was observed by Chadid at 4676.5 Å at phase 0.94 (see her Fig. 7). Consequently, it is quite plausible that Chadid's emission was due to a cosmic ray rather than stellar He II.

The presence or the absence of helium emission lines can be considered as an indication of the shock intensity. Likewise, if the metallic lines are not double, but present only a linewidth broadening, this may give us a clue to the strength of the shock. The minimum energy required for exciting a neutral helium atom is 19.73 eV. This means that if we observe helium emission lines, then the temperature in the de-excitation region of the shock wake is higher than 10 000 K, typically 20 000 K when the He I and H I line strengths are similar. This is much more than the minimum temperature of 229 082 K required to excite He I as assumed by Chadid (2011).

The observation of He II at $\lambda\lambda$4686, which is supposed to form in the shock wake, requires that the minimum temperature would be higher than 30 000 K, typically around 40 000 K to have a greater line strength than those of He I lines. This is much lower than the temperature of 285 367 K expected by Chadid (2011), which corresponds to the minimal energy required for the ionization of a neutral helium atom (24.59 eV).

Basically, because of the tail of the Maxwellian distribution, excitations or ionizations begin below the threshold energies (or temperatures) adopted by Chadid (2011). Accordingly, Chadid seems to have misunderstood the physical conditions when helium emission lines occur, in addition to their detectability in the spectrum of S Ara.

8. Origin of the lump

Until now, the lump was observed in the light curve of a single star: CoRoT ID 0101370131 (Chadid & Preston 2013). In their Fig. 3, the pulsation phase of the light maximum occurs at φ = 0.87 instead of 0.0. Consequently, the correct phase of the lump is φ = 0.48 instead of 0.35. Thus, the lump appears later than the third Hα emission (the "third apparition"). Finally, it is not clear whether the lump is connected with the third emission.

During his investigation of the shock phenomena in the atmosphere of RR Lyrae, Fokin (1992) found that when stellar contraction begins, the hydrogen recombination front (HRF) stops because of constantly increasing density. At this moment, the velocity discontinuity at the HRF transforms into two running waves moving in opposite directions. The downward propagating wave heats the subphotospheric gas, which induces a luminosity increase. For this reason, a small bump should appear on the light curve if the intensity of the phenomenon is strong enough. This may be what happens with CoRoT ID 0101370131.

9. The bulge phenomenon

Chadid & Preston (2013) presented heliocentric radial velocity curves for ten field RRab stars, half of them Blazhko stars.

These curves have already been published by For et al. (2011) but with the complete set of data obtained. Individual spectra were constructed from 13 echelle orders covering the spectral region 4000–4600 Å. Radial velocities were derived by cross-correlation with the template of a blue metal-poor RV standard star that possesses a spectrum similar to those of RR Lyr stars at most phases (For et al. 2011). Thus, these velocities refer to velocities in the metal line-forming layers located above the photosphere. Obviously, because of the Blazhko effect, the velocity dispersion is lower for non-Blazhko stars.

For some stars, Chadid & Preston (2013) claim to observe a swelling of the radial velocity curve around pulsation phase 0.35. They call this effect the "bulge phenomenon". Among the five non-Blazhko stars of their sample, the presence of the bulge is not obvious. Only Z Mic seems affected by the phenomenon, but it is not clearly demonstrated by the observations if we consider the measurement accuracy and the changes during different pulsation cycles. One star (CD Vel) seems to have this bulge, but it requires a definitive confirmation by observations of better quality because Chadid & Preston (2013) estimate that the errors present in their data is near $2\,\mathrm{km\,s^{-1}}$. Moreover, it is not clear that CD Vel is a Blazhko star. For the four other Blazhko stars of the survey, it is not easy to distinguish the presence of the bump due to modulations caused by the Blazhko effect (see their Fig. 1). Again, new uninterrupted and ultra-precise time series observations, such as space photometric missions, are required to definitively confirm the bulge.

The bump, the bulge, or other swelling occurring in the radial velocity curve indicate the presence of more or less strong acceleration phases. The bulge is expected around the maximum expansion of the atmosphere ($\varphi \approx 0.35$). Consequently, because the motion of atmospheric layers is not synchronized over the whole thickness of the atmosphere, dense areas followed by rarefaction zones must be present, especially in the uppermost part of the atmosphere. Thus, weak velocity gradients affect the motion of atmospheric layers. Moreover, because irregularities occur from cycle to pulsation cycle, the atmosphere cannot retrieve an identical dynamic state from one pulsation cycle to the next. Under these conditions, it is normal that, during the ascending branch of the radial velocity curve, around phase $\varphi = 0.35$, irregularities in the radial velocity are observed, especially when the pulsation amplitude is large.

Conversely, it should be surprising that such density gradients can cause the supersonic shock wave $\mathrm{Sh_{PM}}$, at the beginning of the infalling motion of the atmosphere. Moreover, its intensity must be strong enough to create the weak observed redshifted emission (the "third apparition") near $\varphi = 0.30$. In this pulsation phase, the atmosphere has reached its maximum extension, and consequently, from an almost stationary state, atmospheric layers slowly start their infalling motion at subsonic speed onto the photosphere. Fokin & Gillet (1997) showed that shocks with a Mach number greater than 4 (shock front velocity $>40\,\mathrm{km\,s^{-1}}$) only occur after $\varphi \approx 0.75$.

Finally, if the bulge in the RV curve is considered as a new representative episode in the atmospheric dynamics of RR Lyrae stars, then it is very long. It begins at $\varphi = 0.15$ and disappears at approximately $\varphi = 0.60$ (see Fig. 3 of Chadid & Preston 2013). It occurs around the maximum radius, for almost half a pulsation period. Thus, this phenomenon affects both the atmospheric expansion and its contraction. Stars that undergo significant atmospheric expansion should present a bulge phenomenon of large amplitude, and stars with the strongest shocks would have the largest bulges. It would be good to confirm these trends with data of good quality.

10. A shock–induced Blazhko effect?

To explain the Blazhko effect, Gillet (2013) suggested that an amplification mechanism of the intensity of the main shock occurs between Blazhko minimum and maximum. Once the shock strength reaches a critical value (at Blazhko maximum), the shock desynchronizes the motion of photospheric layers. Then, from the Blazhko maximum until the minimum, a relaxation phase takes place. During this interval, layers gradually return to their synchronized motion, which occurs again at the next Blazhko minimum.

Chadid & Preston (2013) expected that the opposite situation, i.e., photospheric layers are synchronized from the Blazhko maximum until the minimum. In this case, it is difficult to understand why the main shock, after a gradual rise up to the Blazhko maximum, can induce a synchronized motion of layers? Moreover, to explain the observed Blazhko modulations of the period, temperature, radius, etc., these authors must have assumed that there is an unknown "physical engine" in the atmosphere. In fact, Gillet (2013) suggested that it is simply the existence of a secondary shock, probably induced by the first overtone (Fokin & Gillet 1997), and radiative losses of the main shock, which are at the origin of the different observed modulations.

11. Conclusion

In this paper, we have discussed the physical origin of hydrogen and helium emission lines observed in RR Lyrae stars. From the three successive emission components occurring in the Hα profile during each pulsation cycle, two are produced by the main shock. Just before the maximum luminosity appears the strongest emission. It is blueshifted. It occurs when the main shock emerges from the photosphere, i.e., when the shock is still close to the stellar disk. The second emission is a weak redshifted component, observed later around the pulsation phase $\varphi = 0.30$. At this time, because the shock seems to currently be in approximately half a stellar radius, a P-Cygni type profile is observed. From the theory of radiative shock waves developed by Fadeyev & Gillet (2004), we could estimate that the velocity of the shock front varies from $132\,\mathrm{km\,s^{-1}}$ at $\varphi = 0.902$ to $114\,\mathrm{km\,s^{-1}}$ at $\varphi = 0.927$. From the width of the P-Cygni profile, we found an average shock-front velocity of $78\,\mathrm{km\,s^{-1}}$ during the visibility of the emission around $\varphi = 0.30$. Thus, during about 40% of the pulsation period, the shock travels a distance of more than 50% of the photospheric radius.

A similar pair (blueshifted and redshifted) of emission components is observed in long-period Cepheids. Until now, no satisfactory explanation of their physical origin has been proposed. In fact, it appears that the same process of propagation of the main shock occurring in the atmosphere of RR Lyrae stars also applies in long-period Cepheids. However, for these stars, the shock travels a much greater distance, up to more than twice the photospheric radius. From the P-Cygni profile of ℓ Carinae, we found a decreasing shock front velocity from 100 to $70\,\mathrm{km\,s^{-1}}$ between the pulsation phases 0.0 and 0.50. From the blueshifted emission, we obtained a shock front velocity of $162\,\mathrm{km\,s^{-1}}$.

To date, spectroscopic observations indicate that He II emission occurs only in Blazhko stars. However, because too few stars have been inspected, we must wait for a survey to be carried out to confirm this trend.

Acknowledgements. We wish to thank Philippe Mathias and Elisabeth Guggenberger for helpful comments and valuable discussions that helped to improve the clarity of the paper. We are grateful to the anonymous referee for the

very thoughtful report that led to improving the text. We gratefully acknowledge Joli Adams for her very careful reading of the paper and valuables suggestions.

References

Abt, H. A. 1959, A&A, 130, 824
Baker, N., & Kippenhahn, R. 1965, ApJ, 142, 868
Baldry, I. K., Taylor, M. M., Bedding, T. R., et al. 1997, MNRAS, 289, 979
Castor, J. P. 1967, Ph.D. Thesis, Pasadena, California
Castor, J. P. 1972, The Evolution of Population II Stars, Proc. a conference held at the State University of New York at Stony Brook, December 1970, ed. A. G. D. Philip, Dudley Observatory Report No. 4, 1972, 147
Chadid, M. 2011, RR Lyrae Stars, Metal-Poor Stars, and the Galaxy, Carnegie Observatories Astrophysics Series, ed. A. McWilliam, Pasadena, CA: The Observatories of the Carnegie Institution of Washington, 5, 29
Chadid, M., & Preston, G. W. 2013, MNRAS, 434, 552
Christy, R. F. 1964, Rev. Mod. Phys., 36, 555
Christy, R. F. 1966, ApJ, 144, 108
Christy, R. F. 1967, IAU Symp., 28, 105
Fadeyev, Yu. A., & Gillet, D. 2001, A&A, 368, 901
Fadeyev, Yu. A., & Gillet, D. 2004, A&A, 420, 423
Fokin, A. B. 1991, MNRAS, 250, 258
Fokin, A. B. 1992, MNRAS, 256, 26
Fokin, A. B., Gillet, D., & Breitfellner, M.G. 1996, A&A, 307, 503
Fokin, A. B., & Gillet, D. 1997, A&A, 325, 1013
For, B.-Q., Preston, G. W., & Sneden, C. 2011, ApJ, 194, 38
Geroux, C. M., & Deupree, R. G. 2011, ApJ, 731, 18
Geroux, C. M., & Deupree, R. G. 2013, ApJ, 771, 113
Gillet, D. 2013, A&A, 554, A46
Gillet, D., & Crowe, R. A. 1988, A&A, 199, 242
Gillet, D., Fabas, N., & Lèbre, A. 2013, A&A, 553, A59
Hill, S. J. 1972, ApJ, 178, 793
Hutchinson, J. L., Hill, S. J., & Lille, C. F. 1975, AJ, 80, 1044
Kolenberg, K. 2013, RR Lyrae Studies with Kepler, Stellar Pulsations, Astrophysics and Space Sci. Proc. (Berlin Heidelberg: Springer-Verlag), 31, 109
Ludwig, H.-G., & Kucinskas, A. 2012, A&A, 547, A118
Marconi, M. 2009, Stellar Pulsation: Challenges for Theory and Observation: AIP Conf. Proc., eds. A. Guzik, & P. A. Bradley, 1170, 223
Mundprecht, E., Muthsam, H. J., & Kupka, F. 2013, MNRAS, 435, 3191
Nardetto, N., Groh, J. H., Kraus, S., et al. 2008, A&A, 489, 1263
Preston, G. W. 1964, ARA&A, 2, 23
Preston, G. W. 2009, A&A, 507, 1621
Preston, G. W. 2011, AJ, 141, 6
Preston, G. W., & Paczynski, B. 1964, ApJ, 140, 181
Preston, G. W., Smak, J., & Paczynski, B. 1965, ApJS, 12, 99
Sanford, R. 1949, A&A, 109, 208
Schwarzschild, M. 1952, Transaction of the IAU VIII, ed. P. Th. Oosterhoff (Cambridge University Press), 811
Stellingwerf, R. F. 2013, 40 Years of Variable Stars: A Celebration of Contributions by H. A. Smith, Conf. Proc. Regional Variable Star Conference 30–31 May 2013 East Lansing, Michigan, eds. K. Kinemuchi, C. A. Kuehn, N. De Lee, & H. A. Smith, 28
Tuggle, R. S., & Iben, I. J. 1973, ApJ, 186, 593
Wallerstein, G. 1959, A&A, 130, 560
Wedemeyer, S., Freytag, B., Steffen, M., et al. 2004, A&A, 414, 1121
Whitney, C. 1956a, Ann. Astrophys., 19, 34
Whitney, C. 1956b, Ann. Astrophys., 19, 142